Model Uncertainty in Accelerated Degradation Testing Analysis

Le Liu, Xiao-Yang Li, Enrico Zio, Rui Kang, Tong-Min Jiang

Model Uncertainty in Accelerated Degradation Testing Analysis

Le Liu, Xiao-Yang Li, Enrico Zio, *Senior Member, IEEE*, Rui Kang, and Tong-Min Jiang

***Abstract*—In accelerated degradation testing (ADT), test data from higher than normal stress conditions are used to find stochastic models of degradation, e.g., Wiener process, Gamma process, and inverse Gaussian process models. In general, the selection of the degradation model is made with reference to one specific product and no consideration is given to model uncertainty. In this paper, we address this issue and apply the Bayesian model averaging (BMA) method to constant stress ADT. For illustration, stress relaxation ADT data are analyzed. We also make a simulation study to compare the s-credibility intervals for single model and BMA. The results show that degradation model uncertainty has significant effects on the p-quantile lifetime at the use conditions, especially for extreme quantiles. The BMA can well capture this uncertainty and compute compromise s-credibility intervals with the highest coverage probability at each quantile.**

***Index Terms*—Accelerated aging, Bayesian methods, degradation, stochastic processes, uncertainty.**

NOMENCLATURE

A. Acronyms

ALT	Accelerated life test(ing).
ADT	Accelerated degradation test(ing).
AIC	Akaike's information criterion.
BMA	Bayesian model averaging.
D–S	Dempster–Shafer
MLE	Maximum-likelihood estimator.
MCMC	Markov chain Monte Carlo.
USP	Unified stochastic degradation model.
PDF	Probability density function.
CDF	Cumulative density function.
FPT	First passage time.
BISA	Birnbaum–Saunders-type distribution.
CP	Coverage probability.
AL	Average interval length.

B. Notation

$X(t)$	Product degradation path.
$\Lambda(t)$	Age function of time t.
γ	Time-scale parameter.
μ, σ	Degradation parameters.
α_0, α_1	Acceleration parameters.
$a(t)$, $b(t)$	Parameters in the unified model.
c, C	Candidate model c, number of models.
D	ADT dataset.
$f_N(\cdot)$	PDF of normal distribution.
$f_{Ga}(\cdot)$	PDF of Gamma distribution.
$f_{IG}(\cdot)$	PDF of inverse Gaussian distribution.
i, j, k	ith stress level, unit j, measurement k.
K	Number of stress levels.
n_i	Test samples under the ith stress level.
m_{ij}	Number of measurements for unit j under the ith stress level.
s, s'	Stress level.
$L(\cdot)$, $l(\cdot)$	Likelihood and log-likelihood function.
$\boldsymbol{\theta}_c$, $\hat{\boldsymbol{\theta}}_c$, $\widetilde{\boldsymbol{\theta}}_c$	Vector of parameters.
ω	Failure threshold.
p, z	Quantile.
t_p, t_{pc}, $\hat{t}_{pc}$	p-quantile lifetime at the use condition.
q	Confidence level.
∇t_p	First derivative of t_p.
$AVar(\cdot)$	Asymptotic variance.
$\boldsymbol{I}$, $\boldsymbol{I}^{-1}$	Fisher information matrix, its inverse.
$\Gamma(\cdot)$	Gamma function.
$\psi(\cdot)$, $\psi_1(\cdot)$	Digamma and trigamma function.
$P(\cdot)$	Model probability.

Manuscript received November 6, 2016; revised February 16, 2017; accepted April 9, 2017. Date of publication May 12, 2017; date of current version August 30, 2017. This work was supported in part by the National Natural Science Foundation of China under Grant 61603018, Grant 61104182, and Grant 61573043, and in part by the Fundamental Research Funds for the Central Universities under Grant YWF-16-JCTD-A-02-06. Associate Editor: S. Li. *(Corresponding author: Xiao-Yang Li.)*

L. Liu, X.-Y. Li, and R. Kang are with the School of Reliability and Systems Engineering, Beihang University, Beijing 100191, China, and also with the Science and Technology on Reliability and Environmental Engineering Laboratory, Beijing 100191, China (e-mail: liule89@gmail.com; leexy@buaa.edu.cn; kangrui@buaa.edu.cn).

E. Zio is with the Department of Energy, Politecnico di Milano, Milano 20133, Italy, and also with the Chair on System Science and the Energetic Challenge, Foundation Electricite de France, CentraleSupelec, Universite Paris-Saclay, Paris 92295, France (e-mail: enrico.zio@ecp.fr).

T.-M. Jiang is with the School of Reliability and Systems Engineering, Beihang University, Beijing 100191, China (e-mail: jtm@buaa.edu.cn).

Color versions of one or more of the figures in this paper are available online at http://ieeexplore.ieee.org.

Digital Object Identifier 10.1109/TR.2017.2696341

I. INTRODUCTION

MANY products are designed to be highly reliable and to have a long lifespan, e.g., battery life of 15 years for hybrid electric vehicles [1]. Traditional reliability tests are obviously not suitable for the reliability assessment of such products over such long time spans. Thus, accelerated degradation tests (ADT) are widely used to accelerate the failure/degradation processes by exposing the products to severe test conditions. Successful applications of ADT have been developed for batteries [2], light-emitting diodes [3], metal–oxide–semiconductor field-effect transistors [4], smart electricity meter [5], and others.

In standard ADT data analysis, a degradation model is assumed to describe the degradation paths of the samples tested at different stress levels and some specific parameters of the model are assumed to be stress related, as described by a given acceleration model, e.g., the drift coefficient in the Wiener process [6]–[8]. In general, acceleration models are assumed based on the physical mechanisms of the tested samples or empirical observations of the stress variable [9], e.g., temperature-Arrhenius model, voltage-Eyring model, etc. After obtaining the data from ADT, inference on unknown parameters is taken up, both of the degradation and acceleration models. Then, the product reliability assessment and lifetime evaluation are performed with the estimated parameters under the given use conditions. Statistical inference methods for ADT data analysis have been extensively reviewed in [10] and [11].

In the literature, stochastic process models has drawn more attention than degradation-path models due to their ability to describe temporal variability [12], like the Wiener process model [13], [14], Gamma process model [15]–[18], and inverse Gaussian process model [19]–[22]. The Wiener process model is often used when the degradation process is fluctuating with time. If the degradation process is nondecreasing, both Gamma and inverse Gaussian process models are generally used in preference to the Wiener process model and to ensure the monotonous property. However, in some engineering applications, the Wiener process model is also used to deal with monotonous data. Examples are given in [23]–[25].

For a given ADT dataset, more than one model might be plausible to describe it. Thus, model uncertainty exists in standard ADT data analysis, which has not been considered and that may lead to wrong inferences. Also, in ALT, different lifetime distributions may plausibly describe the time to failure data and the problem of model uncertainty arises. This is, for example, treated in [26] by the BMA method, with demonstration that the choice of the distribution has significant effects on the results of the lifetime evaluation at the use conditions, especially for extreme quantiles. For ADT, the AIC has been introduced to select the appropriate model [7], [27]. However, the effect of model uncertainty on the lifetime evaluation results is not considered. In [28], both Wiener and Gamma process models have been used, and shown to give accurate parameter estimates. However, the question remains to how the degradation model affects the lifetime evaluation results and how the model uncertainty can be accounted for.

Although it would be possible account both for accelerating and degradation models uncertainty, as mentioned in [26], this can result in a very complicated extrapolation. Hence, following [26] in this paper, we consider only the uncertainty about the degradation models by analyzing three stochastic process models commonly used in ADT.

With respect to model uncertainty in literature, many works have addressed this issue [29]–[31]. In [32], two approaches, i.e., alternate hypotheses (also known as model averaging) and adjustment factor, have been used to treat model uncertainty by expert judgments. The former one combines all the available models through a mixture of probabilities. The latter selects a best model as reference and updates it with information from the other models. Model averaging has been fully extended into BMA [33]–[36], by the integration of model prior knowledge and the likelihood function of the obtained data for each model. In [37], it is applied to account for model uncertainty based on the differences between experimental observations and model predictions.

One problem of the model averaging method is that it assumes that the real model is one of the candidate models since the summation of model probabilities must be equal to one, even though it is unknown and of difficult interpretation, and controversial in practical applications. To relax this assumption, D–S theory can be introduced, using belief and plausibility functions to account for model uncertainty [38], [39]. Some difficulties may arise in this method for the elicitation of expert knowledge on the belief values to assign to the models.

As to the adjustment-factor method, some work has been done for its application to accelerated testing models based on field lifetime or degradation data. For example, Wang *et al.* [40] chose exponential and Weibull lifetime distributions as the reference models for Device-A ALT data; then, a calibration factor is introduced to update the reference models with the field failure data since the lab-test environment and field conditions are different. A similar procedure is used for ADT models in [41].

In this paper, we contribute to accounting for model uncertainty in the lifetime evaluation from ADT data. The BMA method is selected due to its mathematical soundness and computational convenience. For the application of BMA, we assume that the three degradation models are an exhaustive set within which the real model lies. An alternative could be to the D–S theory with expert knowledge or the adjustment-factor method based on field information, but these are not within the scope of this paper, and will be considered in future works.

The rest of the paper is organized as follows. In Section II, a unified stochastic process (USP) model is defined to comprise the three candidate models and the statistical inferences. The MLE and its s-confidence interval for p-quantile lifetime estimation at the use conditions are also proposed. The lifetime is determined assuming that the considered degrading units fail when the degradation levels exceed a given threshold, called the failure threshold. In Section III, the BMA method for model uncertainty analysis is introduced and MCMC is implemented for its numerical resolution. In Sections IV and V, an illustrative example is presented to show the implementation of the method proposed in the preceding sections. Finally, some concluding remarks are given in Section VI.

II. The USP Model for ADT Evaluation

A. Unified Stochastic Degradation Model

In standard ADT analysis, it is customary to assume that the degradation $X(t)$ follows a process with statistically independent increments, where the mean and variance of $X(t)$ are proportional to the age function of time as $\Lambda(t)$, and $\Lambda(t)$ is a nonnegative increasing function. Herein, a unified stochastic process $X(t) = \text{USP}(t)$ is a process with statistically independent increments such that the mean and variance functions have the form

$$E(X(t)) = \mu\Lambda(t) \tag{1}$$

$$\text{Var}(X(t)) = \sigma^2\Lambda(t) \tag{2}$$

where $\mu, \sigma^2 > 0$ and $\Lambda(t)$ is a nonnegative increasing function. If for any fixed $t > 0$, the PDF of $X(t)$ depends on two parameters $a(t)$ and $b(t)$, which are values of positive time functions a and b, then, we use notation $X(t) = \text{USP}(a(t), b(t))$, shortly $X = \text{USP}(a, b)$. Taking into account that the mean and the variance are functions of $a(t)$ and $b(t)$, equalities (1) and (2) imply that these functions can be written in terms of μ, σ^2 and $\Lambda(t)$.

For instance, the unified stochastic process model becomes the Wiener process model when $X(t) \sim N(a(t), b(t))$, where $a(t) = \mu\Lambda(t)$ is the mean value and $b(t) = \sqrt{\sigma^2\Lambda(t)}$ is the standard deviation. For any fixed $t > 0$, the PDF of $X(t)$ is $f_N(x|a(t), b(t))$, where

$$f_N(x \mid a(t), b(t)) = \frac{1}{\sqrt{2\pi}b(t)} \exp\left[-\frac{(x - a(t))^2}{2b(t)^2}\right]. \quad (3)$$

The unified stochastic process model becomes the Gamma process model when $X(t) \sim Ga(a(t), b(t))$, where $a(t) = \frac{\mu^2\Lambda(t)}{\sigma^2}$ is the shape parameter and $b(t) = \frac{\sigma^2}{\mu} > 0$ is the scale parameter. For any fixed $t > 0$, the PDF of $X(t)$ is $f_{Ga}(x|a(t), b(t))$, where

$$f_{Ga}(x \mid a(t), b(t)) = \frac{b(t)^{-a(t)}}{\Gamma(a(t))} x^{a(t)-1} \exp\left(-\frac{x}{b(t)}\right), x > 0. \quad (4)$$

The unified stochastic process model becomes the inverse Gaussian process model when $X(t) \sim IG(a(t), b(t))$, where $a(t) = \mu\Lambda(t)$ is the mean parameter and $b(t) = \frac{\mu^3\Lambda^2(t)}{\sigma^2} > 0$ is the shape parameter. For any fixed $t > 0$, the PDF of $X(t)$ is $f_{IG}(x|a(t), b(t))$, where

$$f_{IG}(x \mid a(t), b(t)) = \sqrt{\frac{b(t)}{2\pi x^3}} \exp\left[-\frac{b(t)(x - a(t))^2}{2a(t)^2 x}\right], x > 0. \quad (5)$$

Through the above definitions, we can analyze the influence of the degradation model uncertainty on the p-quantile lifetime at the use conditions.

B. Acceleration Model With Normalized Stress

The acceleration model describes the relationship between the accelerated stress s_i' and the degradation rate μ_i. It can be obtained based on either physical knowledge of the tested products or empirical observations. The typical physics-based acceleration models include the Arrhenius model, Eyring model, etc. [9], while the empirical acceleration models include the Coffin–Manson model [42], etc. A general log-linear form of the model can be written as

$$\mu_i = \exp(\alpha_0 + \alpha_1 s_i) \quad (6)$$

where α_0 and α_1 are two constant parameters, and s_i is the normalized accelerated stress level given by [8]

$$s_i = \begin{cases} \dfrac{1/s_0' - 1/s_i'}{1/s_0' - 1/s_H'} & \text{Arrhenius relation} \\ \dfrac{lns_i' - lns_0'}{lns_H' - lns_0'} & \text{power law relation} \\ \dfrac{s_i' - s_0'}{s_H' - s_0'} & \text{exponential relation} \end{cases} \quad (7)$$

where s_0' and s_H' are the normal and highest stress levels, respectively. Formulas (7) imply $s_0 = 0$, $s_H = 1$, $s_i \in [0, 1], i = 1, 2, \ldots, K$, and the degradation rate at the use conditions is $\mu_0 = \exp(\alpha_0)$.

C. Statistical Inference

For the constant stress scenario, we assume that $X(t_{ijk})$ is the kth degradation value of unit j under the ith stress level and t_{ijk} is the corresponding measurement time, $i = 1, 2, \ldots, K, j = 1, 2, \ldots, n_i, k = 1, 2, \ldots, m_{ij}$, where K is the number of stress levels, n_i is the number of test samples under the ith stress level, and m_{ij} is the number of measurements for unit j under the ith stress level.

Let $x_{ijk} = X(t_{ijk}) - X(t_{ij(k-1)})$ be the observed degradation increment and $\Lambda_{ijk} = \Lambda(t_{ijk}) - \Lambda(t_{ij(k-1)})$ the corresponding increment of the age function. In addition, the exponential form of $\Lambda(t) = t^\gamma$ is used for time-scale transformation: when $\gamma = 1$, a linear function is given for the time; otherwise, it is nonlinear.

From the definitions in (3)–(5), the likelihood function of the ADT data D is given as

$$L(D|\boldsymbol{\theta}) = \prod_{i=1}^{K} \prod_{j=1}^{n_i} \prod_{k=1}^{m_{ij}} f_{\text{USP}}(x_{ijk}|a_{ijk}, b_{ijk}) \quad (8)$$

where the unknown parameter vector $\boldsymbol{\theta} = [\alpha_0, \alpha_1, \sigma, \gamma]$. The MLE of $\hat{\boldsymbol{\theta}}$ can be easily obtained by maximizing the corresponding log-likelihood function, $l(\boldsymbol{\theta}_c|M_c, D)$ in (9)–(11), as shown at bottom at this page, where we denote by M_1, M_2, and M_3 the candidate Wiener, Gamma, and inverse Gaussian process models, respectively. See (9)-(11) at the bottom of the page.

$$l(\boldsymbol{\theta}_1|M_1, D) = \sum_{i=1}^{K} \sum_{j=1}^{n_i} \sum_{k=1}^{m_{ij}} \left\{ -\frac{1}{2}\ln 2\pi - \frac{1}{2}\ln\sigma^2 - \frac{1}{2}\ln\Lambda_{ijk} - \frac{(x_{ijk} - \mu_i\Lambda_{ijk})^2)}{2\sigma^2\Lambda_{ijk}} \right\} \quad (9)$$

$$l(\boldsymbol{\theta}_2|M_2, D) = \sum_{i=1}^{K} \sum_{j=1}^{n_i} \sum_{k=1}^{m_{ij}} \left\{ -\ln\Gamma\left(\frac{\mu_i^2\Lambda_{ijk}}{\sigma^2}\right) - \frac{\mu_i^2\Lambda_{ijk}}{\sigma^2}\ln\left(\frac{\sigma^2}{\mu_i}\right) + \left(\frac{\mu_i^2\Lambda_{ijk}}{\sigma^2} - 1\right)\ln x_{ijk} - \frac{\mu_i x_{ijk}}{\sigma^2} \right\} \quad (10)$$

$$l(\boldsymbol{\theta}_3|M_3, D) = \sum_{i=1}^{K} \sum_{j=1}^{n_i} \sum_{k=1}^{m_{ij}} \left\{ \frac{3}{2}\ln\mu_i + \ln\Lambda_{ijk} - \frac{1}{2}\ln 2\pi - \frac{1}{2}\ln\sigma^2 - \frac{3}{2}\ln x_{ijk} - \frac{\mu_i (x_{ijk} - \mu_i\Lambda_{ijk})^2}{2\sigma^2 x_{ijk}} \right\} \quad (11)$$

Noted that some degradation trajectories exceed the failure threshold under certain circumstances, which lead to the situation with both degradation and failure time data available. In this paper, we specifically concentrated on the model uncertainty in accelerated degradation testing analysis with degradation data only. For the situation also with failure time data, readers are referred to [27], [40], and [41].

D. p-Quantile Lifetime and Its Variance Through MLE

In the following, the p-quantile lifetime of interest is derived for the unified stochastic process USP(a, b), which can be used for maintenance decision-making or verifying the lifetime and reliability levels of the tested products.

1) p-Quantile Lifetime at the Use Condition: It is easy to verify that in the considered Wiener process the random variable $Y = \Lambda(T)$ has the following inverse Gaussian PDF:

$$Y \sim f_{IG}\left(y \mid \frac{\omega}{\mu}, \frac{\omega^2}{\sigma^2}\right) \tag{12}$$

where T is the FPT (i.e., the time at which the degradation process first exceeds the failure threshold ω). Hence, given that $\Lambda(t)$ is a monotone increasing function, the following CDF is obtained for T

$$F_T(t) = 1 - \Phi\left(\frac{\omega - \mu\Lambda(t)}{\sqrt{\sigma^2\Lambda(t)}}\right) + \exp\left(\frac{2\omega\mu}{\sigma^2}\right)\Phi\left(-\frac{\omega + \mu\Lambda(t)}{\sqrt{\sigma^2\Lambda(t)}}\right) \tag{13}$$

where $\Phi(\cdot)$ denotes the CDF of a standard Normal random variable. The last term in the right-hand side of the equality accounts for the fact that in the Wiener process the events $[X(t) \le \omega$ and $X^*(t) > \omega]$ have a probability strictly greater than zero [43], where $X^*(t) = \sup_{s\in[0,t]} X(s)$. In fact, in the case of the Wiener process the events $T > t$ and $X(t) \le \omega$ are not equivalent. Nonetheless, when $\mu\Lambda(t) \gg \sigma\sqrt{\Lambda(t)}$, this term can be ignored because in this case the Wiener process is practically non-decreasing, and the CDF of the FPT can be approximated as

$$F_T(t) \cong 1 - \Phi\left(\frac{\omega - \mu\Lambda(t)}{\sqrt{\sigma^2\Lambda(t)}}\right). \tag{14}$$

It is possible to show that such approximation is still applicable in the case of the Gamma and inverse Gaussian processes [21], [27].

It is easy to verify that, using this CDF, the following approximate expression can be obtained for the p-quantile of the random variable T at the use condition of interest, μ_0

$$t_p = \Lambda^{-1}\left[\frac{\omega}{4\mu_0}\left(\frac{\sigma}{\sqrt{\omega\mu_0}}z_p + \sqrt{4 + \frac{\sigma^2 z_p^2}{\omega\mu_0}}\right)^2\right] \tag{15}$$

where z_p is the p-quantile of the standard normal distribution and $\Lambda^{-1}(\cdot)$ is the inverse function of $\Lambda(\cdot)$. In fact, assumed that T has the CDF in (14), it results that the variable $Y = \Lambda(T)$ has the following BISA CDF

$$F_Y(y) = \Phi\left[\frac{1}{\alpha}\left(\sqrt{\frac{y}{\beta}} - \sqrt{\frac{\beta}{y}}\right)\right] \tag{16}$$

with $\alpha = \frac{\sigma}{\sqrt{\omega\mu}}$ and $\beta = \frac{\omega}{\mu}$ [27], [43]. Hence, being [44]

$$y_p = \frac{\beta}{4}\left(\alpha z_p + \sqrt{4 + \alpha^2 z_p^2}\right)^2 \tag{17}$$

it results

$$t_p = \Lambda^{-1}(y_p) = \Lambda^{-1}\left[\frac{\beta}{4}\left(\alpha z_p + \sqrt{4 + \alpha^2 z_p^2}\right)^2\right] \tag{18}$$

and thus, being $\alpha = \frac{\sigma}{\sqrt{\omega\mu}}$ and $\beta = \frac{\omega}{\mu}$, writing μ_0 in place of μ, expression (15) is obtained.

2) Approximate Confidence Intervals Based on Fisher Information Matrix: When constructing confidence interval with the MLE information, both empirical (or observed) and expected Fisher information matrixes can be used, see [45] and [46]. In this paper, the expected fisher information matrix is selected. Based on the best asymptotically normal distribution property of the MLE, we get the asymptotic distribution of $\hat{t}_p$

$$\hat{t}_p \approx N\left(t_p, AVar(\hat{t}_p)\right) \tag{19}$$

where $AVar(\hat{t_p})$ is the asymptotic variance of $\hat{t}_p$. The $\widehat{AVar}(\hat{t_p})$ is adopted to obtain the local estimate of $AVar(\hat{t_p})$, that is

$$\widehat{AVar}(\hat{t_p}) = (\nabla t_p)' \boldsymbol{I}^{-1}(\boldsymbol{\theta}_c)\nabla t_p \tag{20}$$

where ∇t_p is the first derivative of t_p in (15) with respect to $\boldsymbol{\theta}_c$, and $\boldsymbol{I}^{-1}(\boldsymbol{\theta}_c)$ is the inverse of the expected Fisher information matrix $\boldsymbol{I}(\boldsymbol{\theta}_c)$ in (21), shown at the bottom of this page. The elements of $\boldsymbol{I}(\boldsymbol{\theta}_c)$ and ∇t_p can be found in the Appendixes A and B, respectively. Meanwhile, the values of those elements will be computed plugging the MLE estimates of unknown parameters $\boldsymbol{\theta}_c$ into (21).

In order to obtain the approximate $100(1-q)\%$ confidence interval for t_p, the logarithmic transformation is commonly

$$\boldsymbol{I}(\boldsymbol{\theta}_c) = \begin{pmatrix} E\left[-\frac{\partial^2 l(\boldsymbol{\theta}_c|M_c,D)}{\partial\alpha_0^2}\right] & E\left[-\frac{\partial^2 l(\boldsymbol{\theta}_c|M_c,D)}{\partial\alpha_0\partial\alpha_1}\right] & E\left[-\frac{\partial^2 l(\boldsymbol{\theta}_c|M_c,D)}{\partial\alpha_0\partial\sigma^2}\right] & E\left[-\frac{\partial^2 l(\boldsymbol{\theta}_c|M_c,D)}{\partial\alpha_0\partial\gamma}\right] \\ & E\left[-\frac{\partial^2 l(\boldsymbol{\theta}_c|M_c,D)}{\partial\alpha_1^2}\right] & E\left[-\frac{\partial^2 l(\boldsymbol{\theta}_c|M_c,D)}{\partial\alpha_1\partial\sigma^2}\right] & E\left[-\frac{\partial^2 l(\boldsymbol{\theta}_c|M_c,D)}{\partial\alpha_1\partial\gamma}\right] \\ & & E\left[-\frac{\partial^2 l(\boldsymbol{\theta}_c|M_c,D)}{\partial(\sigma^2)^2}\right] & E\left[-\frac{\partial^2 l(\boldsymbol{\theta}_c|M_c,D)}{\partial\sigma^2\partial\gamma}\right] \\ & \text{Symmetric} & & E\left[-\frac{\partial^2 l(\boldsymbol{\theta}_c|M_c,D)}{\partial\gamma^2}\right] \end{pmatrix} \tag{21}$$

used [11]

$$\left[\frac{\hat{t}_p}{\exp\left(z_{1-\frac{q}{2}}\frac{\sqrt{\widehat{AVar}(\hat{t}_p)}}{\hat{t}_p}\right)}, \hat{t}_p \exp\left(z_{1-\frac{q}{2}}\frac{\sqrt{\widehat{AVar}(\hat{t}_p)}}{\hat{t}_p}\right)\right]. \tag{22}$$

Note that the aforementioned p-quantile life t_p and its confidence interval are naturally for Gamma and inverse Gaussian process models since they are strictly increasing. However, the Wiener process model is not monotonic that the ignorance of the exponential part will result in larger values of p than the settings (e.g., 0.01, 0.5). Hence, the t_p will become larger with more wider intervals, which is more likely to capture the true values. The results for the Wiener process model in Tables III and IV show that it has acceptable coverage probabilities with wider intervals maybe because of the approximation.

III. Model Uncertainty Through BMA

In this paper, degradation model uncertainty is considered. In order to evaluate the effects of model uncertainty to the p-quantile lifetime, the BMA method is used. This method accounts for model uncertainty by the combination of the inferences from different candidate models [33]. Herein, we briefly recall its basic formulation and, then, propose its computational implementation by the MCMC method.

A. Bayesian Model Averaging

Denoting by $\triangle$ the quantity of interest, i.e., the p-quantile lifetime t_p at the use condition, its posterior distribution given data D is given as

$$f(\triangle|D) = \sum_{c=1}^{C} f(\triangle|M_c, D)P(M_c|D) \tag{23}$$

where $f(\triangle|M_c, D)$ is the posterior density of $\triangle$ assuming that M_c is the correct model and $P(M_c|D)$ is the posterior probability that candidate model M_c is the correct model, which serves as weight in the average and is given by

$$P(M_c|D) \propto f(D|M_c)P(M_c) \tag{24}$$

where $P(M_c)$ is the prior probability that M_c is the correct model and $f(D|Mc)$ is the integrated likelihood of model M_c. Let $\boldsymbol{\theta}_c$ denote the parameter vector of model M_c, with parameter prior $f(\boldsymbol{\theta}_c|M_c)$; the integrated likelihood of D in (24) is, then, given by

$$f(D|M_c) = \int L(D|\boldsymbol{\theta}_c, M_c) f(\boldsymbol{\theta}_c|M_c) d\boldsymbol{\theta}_c \tag{25}$$

where $L(D|\boldsymbol{\theta}_c, M_c)$ is the likelihood function for model $M_c, c = 1, 2, \ldots, C$(=3, in our case).

B. MCMC Implementation

The integral forms in (24) and (25) cannot be easily computed unless the closed form of the integrated likelihood function is available. In order to implement the BMA for model uncertainty analysis, the MCMC method is developed to generate samples from the parameter posterior distribution $f(\boldsymbol{\theta}_c|D, M_c)$ through the following procedures, using the software WinBUGS [47]. Then, the p-quantile at the use conditions can be obtained by (15) from the selected samples.

TABLE I
MLE Estimates and Standard Errors of the Unknown Parameters in the USP

Model	α_0	std	α_1	std	σ	std	γ	std	$l_{\max}$	AIC
M_1	−2.2811	0.2411	2.0047	0.2064	0.4538	0.0360	0.4726	0.0173	−225.3	458.5
M_2	−1.6391	0.1841	1.4323	0.1387	0.4685	0.0367	0.4518	0.0161	−215.9	**439.8**
M_3	−1.5954	0.1740	1.4098	0.1223	0.5185	0.0497	0.4484	0.0158	−217.6	443.1

1) Model Prior Probability $P(M_c)$: The setting of the model prior probability can be based on either expert knowledge or previous ADT of the same kind of products. In practice, one sets this probability to be uniformly distributed if no such prior information is available, i.e., $P(M_c) = \frac{1}{3}, c = 1, 2, 3$.

2) Parameter Prior $f(\boldsymbol{\theta}_c|M_c)$: The parameter vector $\boldsymbol{\theta}_c$ is $[\alpha_{oc}, \alpha_{1c}, \sigma_c, \gamma_c]$. Here, informative priors are adopted, which allow using available prior information. In fact, considered that high temperature stress levels are expected to result in accelerating the degradation process, that is to say, increasing μ, it is possible to say that α_{1c} should be likely greater than zero. As to γ, which regulates the degradation trend, a nonlinear fitting with simply $x = \mu t^{\gamma}$ for each degradation path can provide the necessary prior information. Note that both σ_c and γ are positive parameters. In fact, σ_c is the scale coefficient of the standard deviation of the degradation process and γ is the power of the age function $\Lambda(t) = t^{\gamma}$, that is increasing. Indeed, in the considered unified degradation model, both mean and variance functions have nondecreasing increments, see (1) and (2). Hence, the s-independent and informative prior is assigned, based on the MLE results $\hat{\boldsymbol{\theta}}_c$ from Section II-C

$$\begin{aligned} f(\alpha_{0c}|M_c) &\sim f_N(\alpha_{0c}|\hat{\alpha}_{0c}, 0.01) \\ f(\alpha_{1c}|M_c) &\sim f_N(\alpha_{1c}|\hat{\alpha}_{1c}, 0.01) \\ f(\sigma_c|M_c) &\sim f_{Ga}(\sigma_c|100\hat{\sigma}_c^2, 0.01/\hat{\sigma}_c) \\ f(\gamma_c|M_c) &\sim f_N(\gamma_c|\hat{\gamma}_c, 0.01). \end{aligned} \tag{26}$$

Herein, the variances of the priors are set to be 0.01 for the study in Sections IV and V. For other cases, the standard error (std) of the unknown parameters from MLE can assist the setting of this value, see Table I. The precision for parameters in WinBUGS is the reciprocal of the setting variance. To choose the prior distributions for α_{1c} and γ_c, we assume them to be normally distributed but ensure their nonnegative properties with $P(\alpha_{1c} < 0) \approx 0$ and $P(\gamma_c < 0) \approx 0$. Otherwise, one could use the truncated normal, lognormal or Gamma distributions as alternative choices if the assumptions are invalid.

3) Parameter Posterior $f(\boldsymbol{\theta}_c|D, M_c)$: If the ADT data D are obtained, from (8) and (26), the posterior distribution of $\boldsymbol{\theta}_c$ can be given with the standard Bayes' theorem, that is

$$f(\boldsymbol{\theta}_c|D, M_c) \propto f(\boldsymbol{\theta}_c|M_c) \cdot \prod_{i=1}^{K}\prod_{j=1}^{n_i}\prod_{k=1}^{m_{ij}} f_{\text{USP}}(x_{ijk}|a_{ijk}, b_{ijk}). \tag{27}$$

Through (27), the fully conditions of $\alpha_{0c}, \alpha_{1c}, \sigma_c$, and γ_c can be directly derived, and then a Gibbs sampling strategy can be used to draw parameter samples iteratively with WinBUGS software. The convergence property of the sampling chains will be checked by the Gelman–Rubin index, which is the degree of approximating 1 [47]. Applications can be found in [41] and [48]. When it is converged, a fixed number of samples can be generated from the posterior functions of the parameter vector after a burn-in period (e.g., the first 1000 samples), i.e., $\widetilde{\boldsymbol{\theta}}_c^i = [\tilde{\alpha}_{0c}^i, \tilde{\alpha}_{1c}^i, \tilde{\sigma}_c^i, \tilde{\gamma}_c^i], i = 1, 2, \ldots, d$, for the following calculations, e.g., $d = 5000$.

Mentioned that parameter of the priors in (26) are calibrated using MLE estimates based on actual data, and then updated on the basis of the same data used to formulate the likelihood in (27), which is not fully Bayesian approach. However, this procedure can produce posteriors that are similar to priors for the calculation of p-quantile lifetime analysis when the prior information is scarce, and provide satisfactory results [26], [49].

4) Model Posterior Probability $P(M_c|D)$: From (24) with $P(M_c) = 1/3$, the model posterior probability is proportional to the integrated likelihood $f(D|M_c)$, which can be approximated with the samples $\vec{\boldsymbol{\theta}}_c^i = [\vec{\alpha}_{0c}^i, \vec{\alpha}_{1c}^i, \vec{\sigma}_c^i, \vec{\gamma}_c^i], i = 1, 2, \ldots, r$, generated directly from the parameter prior $f(\boldsymbol{\theta}_c|M_c)$ in (26). Then, the model posterior probability is given as

$$P(M_c|D) \propto \frac{1}{r}\sum_{i=1}^{r} L(D|\vec{\alpha}_{0c}^i, \vec{\alpha}_{1c}^i, \vec{\sigma}_c^i, \vec{\gamma}_c^i). \tag{28}$$

5) Model Averaging for p-Quantile Lifetime t_p: We at first calculate the model posterior probabilities $P(M_c|D)$ based on (28). Define that $\text{Sum}_c = \frac{1}{r}\sum_{i=1}^{r} L(D|\vec{\alpha}_{0c}^i, \vec{\alpha}_{1c}^i, \vec{\sigma}_c^i, \vec{\gamma}_c^i)$. Then, $P(M_c|D) = \frac{\text{Sum}_c}{\sum_{c=1}^{C}\text{Sum}_c}$.

Assumed that d groups of parameter samples are generated from $f(\boldsymbol{\theta}_c|D, M_c)$ in (27), i.e., $\widetilde{\boldsymbol{\theta}}_c^i, i = 1, 2, \ldots, d, c = 1, 2, 3$. For single model M_c, its p-quantile lifetime inferences t_{pc} can be constructed based on t_{pc}^is given by substituting $\widetilde{\boldsymbol{\theta}}_c^i$ into (15). After that, the model averaging can be conducted directly based on t_{pc}^is with the model probability $P(M_c|D)$ according to (23), which allows the analysis for both single model and BMA method simultaneously without generating new parameter samples. An algorithm is given below.

Generate parameter samples $\widetilde{\boldsymbol{\theta}}_c^i$ from (27), $i = 1, 2, \ldots, d$, $c = 1, 2, 3$
Set p value
for $i = 1$ **to** d **do**
  Compute $t_{pc}^i, c = 1, 2, 3$, according to (15)
  Generate a random number r_i from the uniform distribution [0,1]
  If $r_i \in [0, Pr(M_1|D)]$, then $t_p^i = t_{p1}^i$; else if $r_i \in [P(M_1|D), \sum_{c=1}^{2} P(M_c|D)]$, then $t_p^i = t_{p2}^i$; otherwise, $t_p^i = t_{p3}^i$
end for

The BMA statistical inferences can be obtained by analyzing the selected t_p^is, e.g., median values, $(1-q)\%$ s-credibility intervals. The BMA results can be compared with t_{pc}^i and also

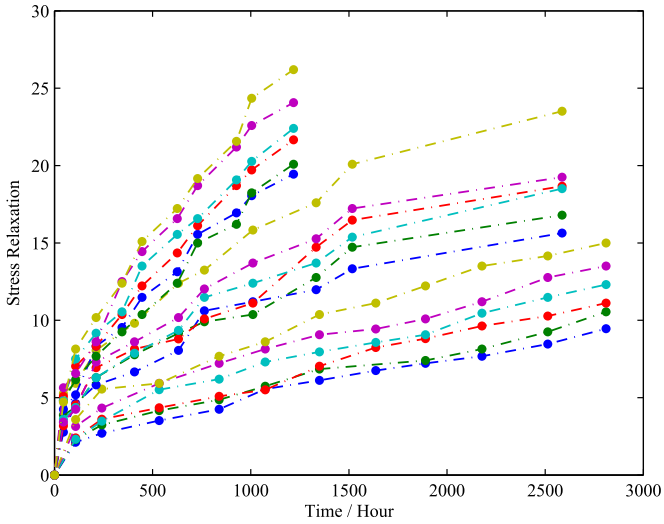

Fig. 1. Stress relaxation data under three temperature stress levels.

MLEs from Section II-D. From the viewpoint of both standard Bayesian and frequentist approaches, this comparison will further verify that in the case considered in the next Section, the p-quantile lifetime evaluation results will lead to overconfident inferences without accounting for model uncertainty in ADT analysis.

IV. Illustrative Example

We use stress relaxation ADT data to illustrate model uncertainty in ADT data analysis and show its influence on p-quantile lifetime evaluation at the use conditions. Stress relaxation is the resistance loss of a component due to a constant strain over time. For instance, the contacts of electrical connectors fail because of the excessive stress relaxation. The data are originated from [50] and listed in [21, Table IV]. Three accelerated temperature stress values have been considered in ADT, i.e., 65, 85, and 100 °C, to collect data for lifetime evaluation at the normal operating temperature of 40°C, see Fig. 1. The electrical connector is said to have failed when the stress relaxation exceeds 30%, i.e., $\omega = 30$.

A. MLE Analysis

In [21], the inverse Gaussian process model is used for ADT modeling and designing optimal test plans without accounting for model uncertainty. Here, the unified degradation model USP(a, b) proposed in Section II-A is used and the MLE results are given in Table I, where the estimated standard errors are computed through the square roots of the diagonal elements of the inverse of the expected Fisher information matrix. Substituting the results into (15) and (22), we can plot the MLE of the quantiles at the use condition and the corresponding 95% s-normal approximation s-confidence intervals with $p = (0.01, 0.05, 0.1, 0.3, 0.5, 0.7, 0.9, 0.95, 0.99)$, see Fig. 2(c) and (d) for t_p in normal scale (some data for M_1 are eliminated to guarantee the presentation) and logarithm scale, which can give an intuitive understanding on the differences of lifetime evaluation among the three candidate models. Meanwhile, Fig. 2(a) and (b) presents the PDF and CDF of FPT.

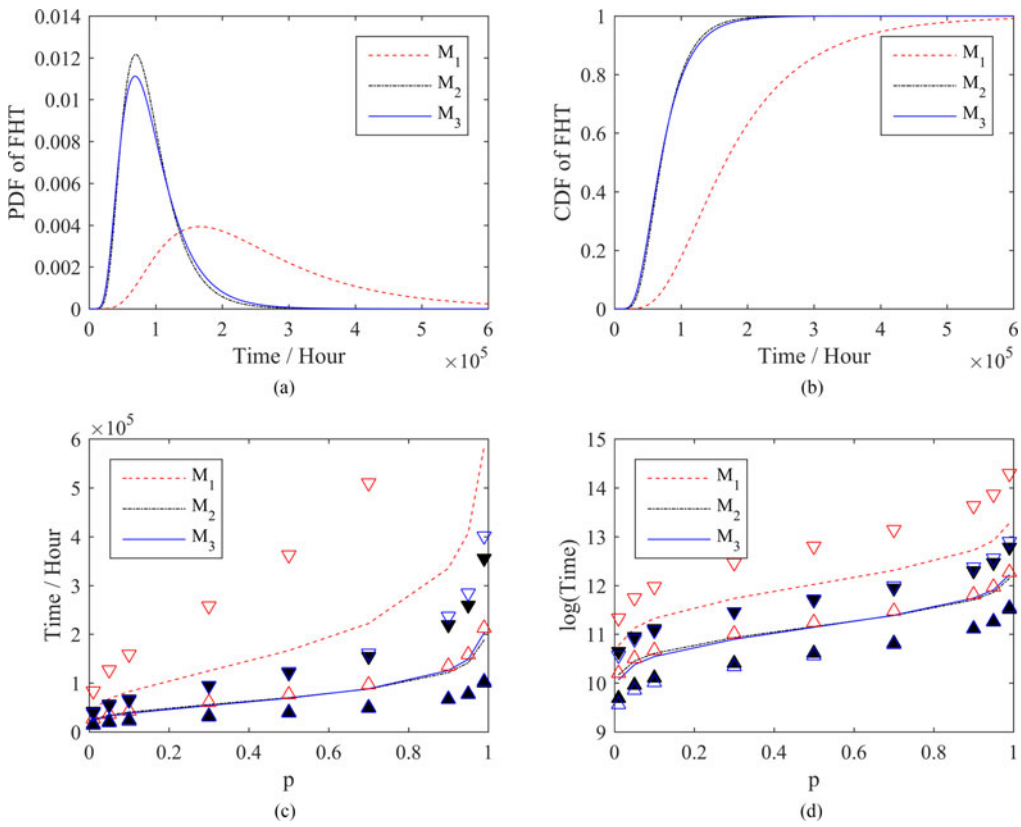

Fig. 2. (a) PDF and (b) CDF for FHT, MLE, and 95% s-confidence intervals for t_p in (c) normal scale and (d) logarithm scale (∇ and $\triangle$ are the upper and lower boundaries, respectively).

Herein, we also compute the expected and empirical Fisher matrixes to understand the differences between them. For M_1, the values are

$$\boldsymbol{I}(\boldsymbol{\theta}_1)_{\text{exp}} = \begin{pmatrix} 849.9045 & 743.0543 & 0 & 6.3226e3 \\ 743.0543 & 673.8037 & 0 & 5.4793e3 \\ 0 & 0 & 2.1816e3 & 3.6469e3 \\ 6.3226e3 & 5.4793e3 & 3.6469e3 & 5.6562e4 \end{pmatrix}$$

and

$$\boldsymbol{I}(\boldsymbol{\theta}_1)_{\text{emp}} = \begin{pmatrix} 849.9045 & 743.0543 & -2.7878e-5 & 6.3226e3 \\ 743.0543 & 672.4577 & -2.7158e-5 & 5.4793e3 \\ -2.7878e-5 & -2.7158e-5 & 2.1816e3 & 3.6469e3 \\ 6.3226e3 & 5.4793e3 & 3.6469e3 & 5.6671e4 \end{pmatrix}$$

respectively. It can be seen that the expected and empirical Fisher matrixes are almost equal, which are also true for M_2 and M_3. Hence, the expected Fisher information matrix is selected to construct the confidence intervals for the p-quantile lifetime.

From Fig. 2(c) and (d), the p-quantiles for model M_1 are larger than the other two models with wider confidence intervals, and the low limit values are even larger than the MLEs of M_2 and M_3. For M_2 and M_3, if the quantiles of interest are at middle quantile ($p = 0.5$), the differences are negligible: $t_{0.5}$ is 7.0036e4 $(4.0623e4, 1.2074e5)$ for M_2 and 6.9066e4 $(3.8742e4, 1.2313e5)$ for M_3. However, the results are very different at extreme quantiles. For instance, the MLE and 95% s-confidence interval of $t_{0.01}$ $(t_{0.99})$ for M_2 are 2.5988e4 (1.8874e5) and (1.6107e4, 4.1932e4) (1.00181e5, 3.5557e5). When it comes to M_3, the results are 2.3457e4 (2.0336e5) and (1.4180e4, 3.8802e4) (1.0313e5, 4.0098e5). In addition, the MLE results for M_3 are smaller than for M_2 at low quantiles ($p < 0.5$). On the contrary, at high quantiles, they are larger than that from M_2.

The above-mentioned analysis has shown that the stochastic model used for ADT analysis can impact the inference results of the p-quantile lifetime. For selecting which model to use, one may use the AIC and choose the model with the lowest AIC value. Given the MLE results in Table I, M_2 would be selected with AIC = 439.8 against M_3 (443.1) and M_1 (458.5). However, such model selection only tells how well a given model fits the data. No information is provided about the influence of model uncertainty on the lifetime evaluation results of interest [26]. It is true that the Gamma process model suits better the stress relaxation data than the other two models. However, the inverse Gaussian process model is artificially chosen in [21] as the underlying degradation model. Such problem may also exist in the other two models for ADT analysis, see [17] and [28]. Hence, model uncertainty should be considered in ADT analysis. For this reason, the BMA method is here used to account for model uncertainty and evaluate its effects on lifetime evaluation.

B. BMA Analysis

Following the procedure in Section III-B, we generated 10 000 samples to compute the posterior probability of each candidate model. The results are $P(M_1|D) = 7.1041e-5$, $P(M_2|D) = 0.8146$, and $P(M_3|D) = 0.1854$. This indicates that the Gamma process model is the best model to represent the stress relaxation ADT data, which is in accordance with

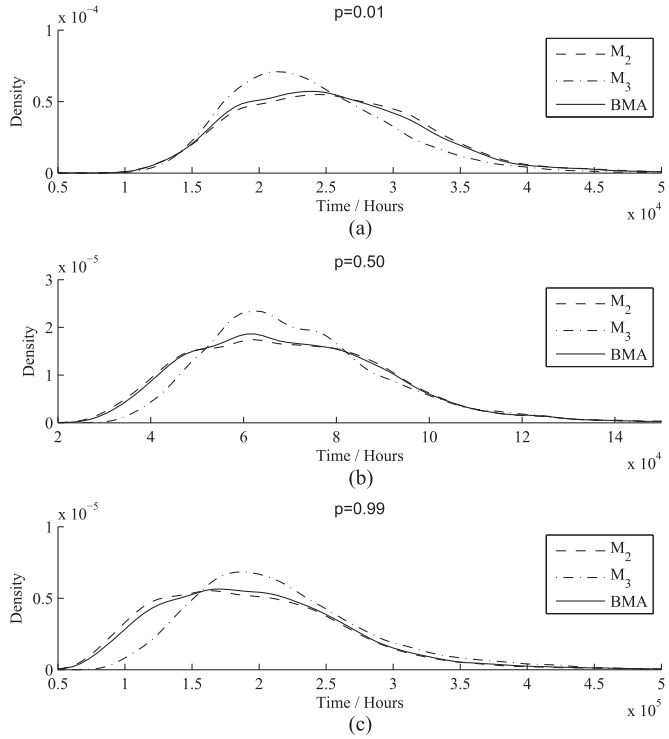

Fig. 3. Posterior density of (a) $t_{0.01}$, (b) $t_{0.50}$, and (c) $t_{0.99}$ [the solid line is for BMA; the dotted and the dashed lines are for Gamma and inverse Gaussian process models, respectively].

the results from MLE and AIC. As shown, the contribution of M_1 is negligible with significantly low posterior probability. Hence, the posterior samples of t_p are computed from M_2 with probability of 0.8146 and from M_3 with probability of 0.1854. For the inferences of quantiles under BMA, the algorithm in Section III-B5 is used and the assigned variances 0.01 of the prior distributions is appropriate to generate prior samples. We plot the middle and extreme quantiles using the $ksdensity$ function in MATLAB, see Fig. 3 for the posterior densities of $t_{0.01}$, $t_{0.50}$, and $t_{0.99}$ under M_2, M_3, and BMA, respectively.

As shown in Fig. 3, the density functions of M_2 and M_3 are different at extreme quantiles, while similar at middle quantile. As expected, most of BMA realizations are from M_2, since M_2 is the best model and, thus, has a larger posterior probability. In order to compare the results from the single model with BMA, we sort the t_{pc}^is from M_2, M_3, and t_p^is of BMA, and compute the posterior median and 95% s-credibility intervals, as reported in Table II. For the median value, the differences are around 1000 h when $p = 0.01$ and 10 000 h when $p = 0.99$, and about 300 h when $p = 0.50$. The results demonstrate that significant differences exist when choosing the degradation model, especially for extreme quantiles, and that BMA, which provides (compromise) point estimates between those of M_2 and M_3, allows computing confidence intervals that account for such uncertainty. The same is true for the 95% s-credibility intervals. From Table II, we see that the lower and upper limit values of BMA are between those of M_2 and M_3: for instance, the lower limit of BMA when $p = 0.01$ is 1.4331e4 h, while that from M_2 and M_3 are 1.4297e4 and 1.4606e4 h, respectively.

TABLE II
POSTERIOR MEDIAN AND 95% s-CREDIBILITY INTERVALS OF M_2, M_3, AND BMA, IN HOURS

Model	Quantile	Median	95% s-credibility interval
M_2	0.01	2.5190e4	[1.4297e4, 4.1077e4]
	0.50	6.8834e4	[3.5687e4, 1.2129e5]
	0.99	1.8666e5	[8.7705e4, 3.6325e5]
M_3	0.01	2.3106e4	[1.4606e4, 3.7888e4]
	0.50	6.8762e4	[4.2084e4, 1.1883e5]
	0.99	2.0607e5	[1.1576e5, 3.8676e5]
BMA	0.01	2.4739e4	[1.4331e4, 4.0745e4]
	0.50	6.8550e4	[3.6661e4, 1.2134e5]
	0.99	1.9122e5	[9.0412e4, 3.6808e5]

Through the analysis from MLE and BMA in Sections IV-A and IV-B, it can be concluded that ignoring model uncertainty may result in significant differences on the p-quantile lifetime estimated from the obtained ADT data. In the next section, a simulation study is given to show the superiority of BMA.

V. SIMULATION STUDY

In this section, we set up a simulation study to compare the BMA s-credibility intervals with those from single model M_c. For simplicity, the MLE results from Table I are treated as the real values to simulate the degradation paths of stress relaxation under three temperature stress levels. The total sample size of n =18 and 36 is simulated to evaluate the effect of sample size on the lifetime evaluation results. Meanwhile, all samples are equally allocated into the three temperature stress levels. Noted that in the presence of negative increments when the Wiener process model M_1 is used for generating ADT data, we assume $P(M_1|D) = 1$, and $P(M_2|D) = P(M_3|D) = 0$.

The generating process for each degradation path $X(t_{ijk})$ at the ith stress level at the time t_{ijk} (see [21, Table V]) is as follows:

1) select the model M_c as the working model;
2) generate x_{ijk} from M_c according to the settings in USP(a, b) from (3)–(5) with the values in Table I, where $\Lambda(t_{ijk}) = t_{ijk}^{\gamma} - t_{ij(k-1)}^{\gamma}$;
3) compute $X(t_{ijk}) = \sum_{k=1}^{m_{ij}} x_{ijk}$.

During each replication, the true values in Table I are used to generate the ADT data. Then, the MLE estimates $\hat{\boldsymbol{\theta}}$ for the generated data are used to calibrate the priors in (26). Herein, the MLE estimates should be around the true values. Therefore, the assumptions of $P(\alpha_{1c} < 0) \approx 0$ and $P(\gamma_c < 0) \approx 0$ are still applicable to ensure their nonnegative property. For instance, $P(\alpha_{13} < 0) = 1.9534e-45 \approx 0$, $P(\gamma_3 < 0) = 3.6628e-06 \approx 0$. After that, model M_c and BMA can compute their corresponding 95% s-credibility intervals at each quantile. Also, the s-confidence and s-credibility intervals from model selection via AIC (M_{AIC}) and the higher posterior probability (M_{HP}) are given to compare the performance of BMA with that from both frequentist and Bayesian viewpoints, through the CP and AL on 1000 replications.

With the settings in Table I, the negative increments exist in almost every replication for M_1, which will make M_1 the only suitable model without model uncertainty. Thus, M_2 and M_3 are used to generate ADT data. However, with other settings, M_1

TABLE III
CP AND AL (IN PARENTHESES) WHEN GAMMA PROCESS IS USED AS THE CORRECT MODEL

	p	0.01	0.05	0.10	0.30	0.50	0.70	0.90	0.95	0.99
M_2	M_1	0.885	0.9	0.903	0.913	0.917	0.918	0.926	0.929	0.931
$n=18$		(2.9870e4)	(4.3774e4)	(5.3855e4)	(8.3371e4)	(1.1307e5)	(1.5333e5)	(2.3716e5)	(2.9167e5)	(4.2764e5)
	M_2	0.937	0.937	0.937	0.933	0.935	0.935	0.933	0.931	0.932
		(2.7051e4)	(3.7601e4)	(4.4983e4)	(6.5799e4)	(8.5977e4)	(1.1256e5)	(1.6630e5)	(2.0048e5)	(2.8371e5)
	M_3	0.774	0.692	0.648	0.543	0.487	0.451	0.411	0.397	0.363
		(4.2364e4)	(6.6893e4)	(8.7336e4)	(1.6483e5)	(2.7970e5)	(5.2803e5)	(1.5672e6)	(2.7246e6)	(7.6146e6)
	M_{HP}	0.937	0.937	0.935	0.932	0.934	0.934	0.933	0.931	0.932
		(2.7116e4)	(3.7717e4)	(4.5140e4)	(6.6106e4)	(8.6461e4)	(1.1332e5)	(1.6771e5)	(2.0236e5)	(2.8692e5)
	M_{AIC}	0.907	0.905	0.908	0.910	0.906	0.907	0.904	0.905	0.904
		(2.7401e4)	(3.7904e4)	(4.5231e4)	(6.5814e4)	(8.5669e4)	(1.1172e5)	(1.6406e5)	(1.9716e5)	(2.7762e5)
	BMA	0.937	0.937	0.935	0.932	0.934	0.934	0.932	0.931	0.933
		(2.7175e4)	(3.7853e4)	(4.5347e4)	(6.6589e4)	(8.7260e4)	(1.1465e5)	(1.7024e5)	(2.0581e5)	(2.9267e5)
M_2	M_1	0.917	0.926	0.928	0.932	0.933	0.939	0.945	0.947	0.95
$n=36$		(1.9739e4)	(2.8443e4)	(3.4638e4)	(5.2391e4)	(6.9848e4)	(9.3013e4)	(1.4014e5)	(1.7017e5)	(2.4360e5)
	M_2	0.945	0.944	0.945	0.944	0.939	0.943	0.943	0.942	0.942
		(1.8002e4)	(2.4883e4)	(2.9679e4)	(4.3115e4)	(5.6015e4)	(7.2892e4)	(1.0666e5)	(1.2794e5)	(1.7940e5)
	M_3	0.693	0.561	0.496	0.37	0.305	0.245	0.183	0.17	0.141
		(2.8843e4)	(4.4880e4)	(5.7742e4)	(1.0200e5)	(1.5748e5)	(2.5212e5)	(5.2715e5)	(7.6365e5)	(1.5427e6)
	M_{HP}	0.944	0.943	0.945	0.944	0.939	0.942	0.942	0.941	0.941
		(1.8005e4)	(2.4890e4)	(2.9690e4)	(4.3138e4)	(5.6053e4)	(7.2957e4)	(1.0679e5)	(1.2811e5)	(1.7968e5)
	M_{AIC}	0.940	0.938	0.938	0.939	0.939	0.939	0.938	0.938	0.934
		(1.8402e4)	(2.5402e4)	(3.0271e4)	(4.3885e4)	(5.6948e4)	(7.4002e4)	(1.0803e5)	(1.2943e5)	(1.8113e5)
	BMA	0.945	0.944	0.945	0.944	0.939	0.943	0.943	0.942	0.942
		(1.8010e4)	(2.4904e4)	(2.9715e4)	(4.3200e4)	(5.6163e4)	(7.3135e4)	(1.0714e5)	(1.2858e5)	(1.8050e5)

TABLE IV
CP AND AL (IN PARENTHESES) WHEN INVERSE GAUSSIAN PROCESS IS USED AS THE CORRECT MODEL

	p	0.01	0.05	0.10	0.30	0.50	0.70	0.90	0.95	0.99
M_3	M_1	0.846	0.864	0.876	0.898	0.904	0.906	0.917	0.922	0.929
$n=18$		(2.9569e4)	(4.4850e4)	(5.6250e4)	(9.0793e4)	(1.2692e5)	(1.7743e5)	(2.8672e5)	(3.6008e5)	(5.4818e5)
	M_2	0.927	0.928	0.93	0.929	0.926	0.916	0.911	0.903	0.897
		(2.3836e4)	(3.2747e4)	(3.8939e4)	(5.6215e4)	(7.2774e4)	(9.4368e4)	(1.3741e5)	(1.6449e5)	(2.2989e5)
	M_3	0.926	0.926	0.928	0.924	0.922	0.922	0.931	0.932	0.933
		(2.3992e4)	(3.3180e4)	(3.9660e4)	(5.8190e4)	(7.6511e4)	(1.0109e5)	(1.5201e5)	(1.8508e5)	(2.6767e5)
	M_{HP}	0.924	0.924	0.926	0.923	0.921	0.920	0.929	0.927	0.929
		(2.3969e4)	(3.3141e4)	(3.9607e4)	(5.8083e4)	(7.6339e4)	(1.0080e5)	(1.5145e5)	(1.8432e5)	(2.6634e5)
	M_{AIC}	0.927	0.923	0.926	0.925	0.920	0.918	0.915	0.916	0.915
		(2.4229e4)	(3.3285e4)	(3.9636e4)	(5.7667e4)	(7.5328e4)	(9.8854e4)	(1.4711e5)	(1.7819e5)	(2.5508e5)
	BMA	0.927	0.925	0.928	0.926	0.925	0.926	0.93	0.931	0.933
		(2.4000e4)	(3.3193e4)	(3.9677e4)	(5.8259e4)	(7.6628e4)	(1.0131e5)	(1.5241e5)	(1.8554e5)	(2.6835e5)
M_3	M_1	0.889	0.912	0.923	0.934	0.944	0.948	0.953	0.955	0.956
$n=36$		(1.9429e4)	(2.8959e4)	(3.5943e4)	(5.6601e4)	(7.7584e4)	(1.0623e5)	(1.6638e5)	(2.0570e5)	(3.0423e5)
	M_2	0.939	0.934	0.928	0.913	0.89	0.871	0.844	0.833	0.809
		(1.5839e4)	(2.1678e4)	(2.5713e4)	(3.6908e4)	(4.7561e4)	(6.1358e4)	(8.8660e4)	(1.0571e5)	(1.4663e5)
	M_3	0.942	0.94	0.94	0.943	0.948	0.947	0.947	0.946	0.947
		(1.6144e4)	(2.2271e4)	(2.6580e4)	(3.8826e4)	(5.0867e4)	(6.6944e4)	(9.9995e4)	(1.2128e5)	(1.7397e5)
	M_{HP}	0.942	0.940	0.940	0.943	0.948	0.947	0.947	0.946	0.947
		(1.6143e4)	(2.2269e4)	(2.6575e4)	(3.8815e4)	(5.0848e4)	(6.6913e4)	(9.9935e4)	(1.2120e5)	(1.7384e5)
	M_{AIC}	0.942	0.938	0.938	0.938	0.936	0.935	0.934	0.931	0.930
		(1.6337e4)	(2.2464e4)	(2.6761e4)	(3.8954e4)	(5.0885e4)	(6.6760e4)	(9.9255e4)	(1.2014e5)	(1.7168e5)
	BMA	0.942	0.94	0.94	0.943	0.948	0.947	0.949	0.947	0.948
		(1.6142e4)	(2.2270e4)	(2.6581e4)	(3.8838e4)	(5.0898e4)	(6.7002e4)	(1.0012e5)	(1.2143e5)	(1.7424e5)

could be used as given in [28]. The results are listed in Tables III and IV, with the model M_c being M_2 and M_3, respectively.

From the simulation study, some results and considerations are shown below.

1) If M_2 is the true model, the CPs of the intervals are lower than 0.8 with model mis-specification of M_3. With the larger values of p, the performance of M_3 is much worse, even less than 0.2 when increasing the sample size. Maybe Fig. 2 can give some explanations: The differences between M_2 and M_3 become wider with larger values of p. When choosing M_3 instead of M_2, such differences become significant that the confidence intervals of M_3 fails to capture the true parameter values of M_2. Hence, the problem of model mis-specification could become serious.
2) If M_3 is the true model, the mis-specification model M_2 performs well with CPs around 0.9 at small sample sizes. From Table IV, the CPs for wrong model M_2 are even

better than that for M_3 with narrower ALs when $p \leq 0.5$ in the case of $n = 18$. The reasons are from the performance of MLE used to calibrate the priors, the approximation of CP and AL values obtained via Monte Carlo simulation and also the physical similarity between this two models as discussed in [20]. However, when increasing the sample size as $n = 36$, the problem of mis-specification becomes serious compared with $n = 18$.

3) Under different scenarios, model M_1 can give satisfactory CPs over 0.84. The reason is that M_1 regards the monotonous degradation paths as if both increasing and decreasing increments exist. Hence, the uncertainty of degradation path (or the property of Wiener process) leads to wider ALs of M_1 than the correct model, and are more likely to capture the real values.
4) From the CPs and ALs in Tables III and IV, BMA performs better than M_{AIC}, and slightly better than M_{HP} with wider intervals that are the compromise results of the candidate models M_c. In addition, BMA has narrower intervals than that from M_1. These results demonstrate the superiority of the BMA method on modeling model uncertainty in ADT analysis.

VI. Conclusion

In traditional ADT analysis, stochastic process models, i.e., Wiener, Gamma and inverse Gaussian processes, are used for degradation modeling and lifetime evaluation of highly reliable and long lifespan products. In this paper, we analyze the effect of stochastic degradation model uncertainty on the p-quantile lifetime at the use conditions, through the BMA method. Analyzing stress relaxation ADT data, we have highlighted that the differences on the p-quantile lifetime estimated by the different models can be significant, especially at extreme quantiles. By a simulation study, we have shown that model uncertainty can be significant and that the BMA method is a good way to treat it, giving compromise s-credibility intervals with highest CP at each quantile.

The main original contributions of this work are as follows.

1) The importance of the stochastic degradation model for ADT data analysis is highlighted and the case study of stress relaxation ADT data is used to demonstrate that significantly different results in lifetime evaluation at the use conditions can be obtained.
2) The problem of degradation model uncertainty has been effectively dealt with by the BMA method, giving satisfactory p-quantile lifetime evaluation results.

The main focus of this paper has been on analyzing the degradation model uncertainty on the p-quantile lifetime evaluation in constant stress ADT data analysis. Future work may extend it to the ADT analysis under other stress profiles, e.g., step-stress and progressive stress. Meanwhile, it is recognized that also model uncertainty in design ADT plans is worth consideration for future work.

Appendix A
Fisher Information Matrix $\boldsymbol{I}(\boldsymbol{\theta}_c)$

The first and second derivatives of μ_i with respect to α_0 and α_1 are $\frac{\partial \mu_i}{\partial \alpha_0} = \frac{\partial^2 \mu_i}{\partial \alpha_0^2} = \mu_i = \exp(\alpha_0 + \alpha_1 s_i)$, $\frac{\partial \mu_i}{\partial \alpha_1} = \frac{\partial^2 \mu_i}{\partial \alpha_0 \partial \alpha_1} = \mu_i s_i = \exp(\alpha_0 + \alpha_1 s_i) s_i$ and $\frac{\partial^2 \mu_i}{\partial \alpha_1^2} = \mu_i s_i^2 = \exp(\alpha_0 + \alpha_1 s_i) s_i^2$. When $\Lambda(t) = t^\gamma$, $\Lambda_{ijk} = t_{ijk}^\gamma - t_{ij(k-1)}^\gamma$, then $\frac{\partial \Lambda_{ijk}}{\partial \gamma} = t_{ijk}^\gamma ln t_{ijk} - t_{ij(k-1)}^\gamma ln t_{ij(k-1)}$.

For the Wiener process model, the derivation of elements $\boldsymbol{I}(\boldsymbol{\theta}_1)$ is given below. Since $E(x_{ijk}) = \mu_i \Lambda_{ijk}$ and $E[(x_{ijk} - \mu_i \Lambda_{ijk})^2] = \sigma^2 \Lambda_{ijk}$, the elements are given in (29)–(38).

For the Gamma process model, the derivation of elements $\boldsymbol{I}(\boldsymbol{\theta}_2)$ is given below. Since $E(x_{ijk}) = \mu_i \Lambda_{ijk}$ and $E[ln x_{ijk}] = \psi(\frac{\mu_i^2 \Lambda_{ijk}}{\sigma^2}) + ln \frac{\sigma^2}{\mu_i}$, the elements are given in (39)–(48), where $\psi(\cdot)$ and $\psi_1(\cdot)$, respectively, are the digamma and trigamma functions [51].

For the inverse Gaussian process model, the derivation of elements $\boldsymbol{I}(\boldsymbol{\theta}_3)$ is as below. Since $E(x_{ijk}) = \mu_i \Lambda_{ijk}$ and $E[\frac{1}{x_{ijk}}] = \frac{1}{\mu_i \Lambda_{ijk}} + \frac{\sigma^2}{\mu_i^3 \Lambda_{ijk}^2}$ [52], the elements are given in (49)–(58):

$$E\left[-\frac{\partial^2 l(\boldsymbol{\theta}_1|M_1,D)}{\partial \alpha_0^2}\right] = \sum_{i=1}^{K}\sum_{j=1}^{n_i}\sum_{k=1}^{m_{ij}} \frac{\mu_i^2 \Lambda_{ijk}}{\sigma^2} \tag{29}$$

$$E\left[-\frac{\partial^2 l(\boldsymbol{\theta}_1|M_1,D)}{\partial \alpha_1^2}\right] = \sum_{i=1}^{K}\sum_{j=1}^{n_i}\sum_{k=1}^{m_{ij}} \frac{\mu_i^2 s_i^2 \Lambda_{ijk}}{\sigma^2} \tag{30}$$

$$E\left[-\frac{\partial^2 l(\boldsymbol{\theta}_1|M_1,D)}{\partial (\sigma^2)^2}\right] = \sum_{i=1}^{K}\sum_{j=1}^{n_i}\sum_{k=1}^{m_{ij}} \frac{1}{2\sigma^4} \tag{31}$$

$$E\left[-\frac{\partial^2 l(\boldsymbol{\theta}_1|M_1,D)}{\partial \gamma^2}\right] = \sum_{i=1}^{K}\sum_{j=1}^{n_i}\sum_{k=1}^{m_{ij}} \left(\frac{1}{2\Lambda_{ijk}^2} + \frac{\mu_i^2}{\sigma^2 \Lambda_{ijk}}\right) \times \left(\frac{\partial \Lambda_{ijk}}{\partial \gamma}\right)^2 \tag{32}$$

$$E\left[-\frac{\partial^2 l(\boldsymbol{\theta}_1|M_1,D)}{\partial \alpha_0 \partial \alpha_1}\right] = E\left[-\frac{\partial^2 l(\boldsymbol{\theta}_1|M_1,D)}{\partial \alpha_1 \partial \alpha_0}\right] = \sum_{i=1}^{K}\sum_{j=1}^{n_i}\sum_{k=1}^{m_{ij}} \frac{\mu_i^2 s_i \Lambda_{ijk}}{\sigma^2} \tag{33}$$

$$E\left[-\frac{\partial^2 l(\boldsymbol{\theta}_1|M_1,D)}{\partial \alpha_0 \partial \sigma^2}\right] = E\left[-\frac{\partial^2 l(\boldsymbol{\theta}_1|M_1,D)}{\partial \sigma^2 \partial \alpha_0}\right] = 0 \tag{34}$$

$$E\left[-\frac{\partial^2 l(\boldsymbol{\theta}_1|M_1,D)}{\partial \alpha_0 \partial \gamma}\right] = E\left[-\frac{\partial^2 l(\boldsymbol{\theta}_1|M_1,D)}{\partial \gamma \partial \alpha_0}\right] = \sum_{i=1}^{K}\sum_{j=1}^{n_i}\sum_{k=1}^{m_{ij}} \frac{\mu_i^2}{\sigma^2} \frac{\partial \Lambda_{ijk}}{\partial \gamma} \tag{35}$$

$$E\left[-\frac{\partial^2 l(\boldsymbol{\theta}_1|M_1,D)}{\partial \alpha_1 \partial \sigma^2}\right] = E\left[-\frac{\partial^2 l(\boldsymbol{\theta}_1|M_1,D)}{\partial \sigma^2 \partial \alpha_1}\right] = 0 \tag{36}$$

$$E\left[-\frac{\partial^2 l(\boldsymbol{\theta}_1|M_1,D)}{\partial \alpha_1 \partial \gamma}\right] = E\left[-\frac{\partial^2 l(\boldsymbol{\theta}_1|M_1,D)}{\partial \gamma \partial \alpha_1}\right] = \sum_{i=1}^{K}\sum_{j=1}^{n_i}\sum_{k=1}^{m_{ij}} \frac{\mu_i^2 s_i}{\sigma^2} \frac{\partial \Lambda_{ijk}}{\partial \gamma} \tag{37}$$

$$E\left[-\frac{\partial^2 l(\boldsymbol{\theta}_1|M_1,D)}{\partial\sigma^2\partial\gamma}\right] = E\left[-\frac{\partial^2 l(\boldsymbol{\theta}_1|M_1,D)}{\partial\gamma\partial\sigma^2}\right] = \sum_{i=1}^{K}\sum_{j=1}^{n_i}\sum_{k=1}^{m_{ij}}\frac{1}{2\sigma^2\Lambda_{ijk}}\frac{\partial\Lambda_{ijk}}{\partial\gamma} \quad (38)$$

$$E\left[-\frac{\partial^2 l(\boldsymbol{\theta}_2|M_2,D)}{\partial\alpha_0^2}\right] = \sum_{i=1}^{K}\sum_{j=1}^{n_i}\sum_{k=1}^{m_{ij}}\psi_1\left(\frac{\mu_i^2\Lambda_{ijk}}{\sigma^2}\right)\frac{4\mu_i^4\Lambda_{ijk}^2}{\sigma^4} - \frac{3\mu_i^2\Lambda_{ijk}}{\sigma^2} \quad (39)$$

$$E\left[-\frac{\partial^2 l(\boldsymbol{\theta}_2|M_2,D)}{\partial\alpha_1^2}\right] = \sum_{i=1}^{K}\sum_{j=1}^{n_i}\sum_{k=1}^{m_{ij}}\psi_1\left(\frac{\mu_i^2\Lambda_{ijk}}{\sigma^2}\right) \times \frac{4\mu_i^4 s_i^2\Lambda_{ijk}^2}{\sigma^4} - \frac{3\mu_i^2 s_i^2\Lambda_{ijk}}{\sigma^2} \quad (40)$$

$$E\left[-\frac{\partial^2 l(\boldsymbol{\theta}_2|M_2,D)}{\partial(\sigma^2)^2}\right] = \sum_{i=1}^{K}\sum_{j=1}^{n_i}\sum_{k=1}^{m_{ij}}\psi_1\left(\frac{\mu_i^2\Lambda_{ijk}}{\sigma^2}\right)\frac{\mu_i^4\Lambda_{ijk}^2}{\sigma^8} - \frac{\mu_i^2\Lambda_{ijk}}{\sigma^6} \quad (41)$$

$$E\left[-\frac{\partial^2 l(\boldsymbol{\theta}_2|M_2,D)}{\partial\gamma^2}\right] = \sum_{i=1}^{K}\sum_{j=1}^{n_i}\sum_{k=1}^{m_{ij}}\psi_1\left(\frac{\mu_i^2\Lambda_{ijk}}{\sigma^2}\right)\frac{\mu_i^4}{\sigma^4} \times \left(\frac{\partial\Lambda_{ijk}}{\partial\gamma}\right)^2 \quad (42)$$

$$E\left[-\frac{\partial^2 l(\boldsymbol{\theta}_2|M_2,D)}{\partial\alpha_0\partial\alpha_1}\right] = E\left[-\frac{\partial^2 l(\boldsymbol{\theta}_2|M_2,D)}{\partial\alpha_1\partial\alpha_0}\right] = \sum_{i=1}^{K}\sum_{j=1}^{n_i}\sum_{k=1}^{m_{ij}}\psi_1\left(\frac{\mu_i^2\Lambda_{ijk}}{\sigma^2}\right) \times \frac{4\mu_i^4 s_i\Lambda_{ijk}^2}{\sigma^4} - \frac{3\mu_i^2 s_i\Lambda_{ijk}}{\sigma^2} \quad (43)$$

$$E\left[-\frac{\partial^2 l(\boldsymbol{\theta}_2|M_2,D)}{\partial\alpha_0\partial\sigma^2}\right] = E\left[-\frac{\partial^2 l(\boldsymbol{\theta}_2|M_2,D)}{\partial\sigma^2\partial\alpha_0}\right] = \sum_{i=1}^{K}\sum_{j=1}^{n_i}\sum_{k=1}^{m_{ij}}-\psi_1\left(\frac{\mu_i^2\Lambda_{ijk}}{\sigma^2}\right) \times \frac{2\mu_i^4\Lambda_{ijk}^2}{\sigma^6} + \frac{2\mu_i^2\Lambda_{ijk}}{\sigma^4} \quad (44)$$

$$E\left[-\frac{\partial^2 l(\boldsymbol{\theta}_2|M_2,D)}{\partial\alpha_0\partial\gamma}\right] = E\left[-\frac{\partial^2 l(\boldsymbol{\theta}_2|M_2,D)}{\partial\gamma\partial\alpha_0}\right] = \sum_{i=1}^{K}\sum_{j=1}^{n_i}\sum_{k=1}^{m_{ij}}\left(\psi_1\left(\frac{\mu_i^2\Lambda_{ijk}}{\sigma^2}\right) \times \frac{2\mu_i^4\Lambda_{ijk}}{\sigma^4} - \frac{\mu_i^2}{\sigma^2}\right)\frac{\partial\Lambda_{ijk}}{\partial\gamma} \quad (45)$$

$$E\left[-\frac{\partial^2 l(\boldsymbol{\theta}_2|M_2,D)}{\partial\alpha_1\partial\sigma^2}\right] = E\left[-\frac{\partial^2 l(\boldsymbol{\theta}_2|M_2,D)}{\partial\sigma^2\partial\alpha_1}\right] = \sum_{i=1}^{K}\sum_{j=1}^{n_i}\sum_{k=1}^{m_{ij}}-\psi_1\left(\frac{\mu_i^2\Lambda_{ijk}}{\sigma^2}\right) \times \frac{2\mu_i^4 s_i\Lambda_{ijk}^2}{\sigma^6} + \frac{2\mu_i^2 s_i\Lambda_{ijk}}{\sigma^4} \quad (46)$$

$$E\left[-\frac{\partial^2 l(\boldsymbol{\theta}_2|M_2,D)}{\partial\alpha_1\partial\gamma}\right] = E\left[-\frac{\partial^2 l(\boldsymbol{\theta}_2|M_2,D)}{\partial\gamma\partial\alpha_1}\right] = \sum_{i=1}^{K}\sum_{j=1}^{n_i}\sum_{k=1}^{m_{ij}}\left(\psi_1\left(\frac{\mu_i^2\Lambda_{ijk}}{\sigma^2}\right) \times \frac{2\mu_i^4 s_i\Lambda_{ijk}}{\sigma^4} - \frac{\mu_i^2 s_i}{\sigma^2}\right)\frac{\partial\Lambda_{ijk}}{\partial\gamma} \quad (47)$$

$$E\left[-\frac{\partial^2 l(\boldsymbol{\theta}_2|M_2,D)}{\partial\sigma^2\partial\gamma}\right] = E\left[-\frac{\partial^2 l(\boldsymbol{\theta}_2|M_2,D)}{\partial\gamma\partial\sigma^2}\right] = \sum_{i=1}^{K}\sum_{j=1}^{n_i}\sum_{k=1}^{m_{ij}}\left(-\psi_1\left(\frac{\mu_i^2\Lambda_{ijk}}{\sigma^2}\right) \times \frac{\mu_i^4\Lambda_{ijk}}{\sigma^6} + \frac{\mu_i^2}{\sigma^4}\right)\frac{\partial\Lambda_{ijk}}{\partial\gamma} \quad (48)$$

$$E\left[-\frac{\partial^2 l(\boldsymbol{\theta}_3|M_3,D)}{\partial\alpha_0^2}\right] = \sum_{i=1}^{K}\sum_{j=1}^{n_i}\sum_{k=1}^{m_{ij}}\frac{9}{2} + \frac{\mu_i^2\Lambda_{ijk}}{\sigma^2} \quad (49)$$

$$E\left[-\frac{\partial^2 l(\boldsymbol{\theta}_3|M_3,D)}{\partial\alpha_1^2}\right] = \sum_{i=1}^{K}\sum_{j=1}^{n_i}\sum_{k=1}^{m_{ij}}\frac{9}{2}s_i^2 + \frac{\mu_i^2 s_i^2\Lambda_{ijk}}{\sigma^2} \quad (50)$$

$$E\left[-\frac{\partial^2 l(\boldsymbol{\theta}_3|M_3,D)}{\partial(\sigma^2)^2}\right] = \sum_{i=1}^{K}\sum_{j=1}^{n_i}\sum_{k=1}^{m_{ij}}\frac{1}{2\sigma^4} \quad (51)$$

$$E\left[-\frac{\partial^2 l(\boldsymbol{\theta}_3|M_3,D)}{\partial\gamma^2}\right] = \sum_{i=1}^{K}\sum_{j=1}^{n_i}\sum_{k=1}^{m_{ij}}\left(\frac{2}{\Lambda_{ijk}^2} + \frac{\mu_i^2}{\sigma^2\Lambda_{ijk}}\right) \times \left(\frac{\partial\Lambda_{ijk}}{\partial\gamma}\right)^2 \quad (52)$$

$$E\left[-\frac{\partial^2 l(\boldsymbol{\theta}_3|M_3,D)}{\partial\alpha_0\partial\alpha_1}\right] = E\left[-\frac{\partial^2 l(\boldsymbol{\theta}_3|M_3,D)}{\partial\alpha_1\partial\alpha_0}\right] = \sum_{i=1}^{K}\sum_{j=1}^{n_i}\sum_{k=1}^{m_{ij}}\left(\frac{9}{2}s_i + \frac{\mu_i^2 s_i\Lambda_{ijk}}{\sigma^2}\right) \quad (53)$$

$$E\left[-\frac{\partial^2 l(\boldsymbol{\theta}_3|M_3,D)}{\partial\alpha_0\partial\sigma^2}\right] = E\left[-\frac{\partial^2 l(\boldsymbol{\theta}_3|M_3,D)}{\partial\sigma^2\partial\alpha_0}\right] = \sum_{i=1}^{K}\sum_{j=1}^{n_i}\sum_{k=1}^{m_{ij}}-\frac{3}{2\sigma^2} \quad (54)$$

$$E\left[-\frac{\partial^2 l(\boldsymbol{\theta}_3|M_3,D)}{\partial\alpha_0\partial\gamma}\right] = E\left[-\frac{\partial^2 l(\boldsymbol{\theta}_3|M_3,D)}{\partial\gamma\partial\alpha_0}\right] = \sum_{i=1}^{K}\sum_{j=1}^{n_i}\sum_{k=1}^{m_{ij}}\left(\frac{\mu_i^2}{\sigma^2}+\frac{3}{\Lambda_{ijk}}\right)\frac{\partial\Lambda_{ijk}}{\partial\gamma} \quad (55)$$

$$E\left[-\frac{\partial^2 l(\boldsymbol{\theta}_3|M_3,D)}{\partial\alpha_1\partial\sigma^2}\right] = E\left[-\frac{\partial^2 l(\boldsymbol{\theta}_3|M_3,D)}{\partial\sigma^2\partial\alpha_1}\right] = \sum_{i=1}^{K}\sum_{j=1}^{n_i}\sum_{k=1}^{m_{ij}}-\frac{3}{2\sigma^2}s_i \quad (56)$$

$$E\left[-\frac{\partial^2 l(\boldsymbol{\theta}_3|M_3,D)}{\partial\alpha_1\partial\gamma}\right] = E\left[-\frac{\partial^2 l(\boldsymbol{\theta}_3|M_3,D)}{\partial\gamma\partial\alpha_1}\right] = \sum_{i=1}^{K}\sum_{j=1}^{n_i}\sum_{k=1}^{m_{ij}}\left(\frac{\mu_i^2 s_i}{\sigma^2}+\frac{3s_i}{\Lambda_{ijk}}\right)\frac{\partial\Lambda_{ijk}}{\partial\gamma} \quad (57)$$

$$E\left[-\frac{\partial^2 l(\boldsymbol{\theta}_3|M_3,D)}{\partial\sigma^2\partial\gamma}\right] = E\left[-\frac{\partial^2 l(\boldsymbol{\theta}_3|M_3,D)}{\partial\gamma\partial\sigma^2}\right] = \sum_{i=1}^{K}\sum_{j=1}^{n_i}\sum_{k=1}^{m_{ij}}-\frac{1}{\sigma^2\Lambda_{ijk}}\frac{\partial\Lambda_{ijk}}{\partial\gamma} \quad (58)$$

$$\frac{\partial t_p}{\partial\alpha_0} = -\frac{1}{\gamma}A^{(2/\gamma-1)}\left(\frac{\sigma z_p}{\exp(\alpha_0)} + B^{-1/2}\frac{\sigma^2 z_p^2}{2\exp(2\alpha_0)}\right) \quad (59)$$

$$\frac{\partial t_p}{\partial\alpha_1} = 0 \quad (60)$$

$$\frac{\partial t_p}{\partial\sigma^2} = \frac{1}{\gamma}A^{(2/\gamma-1)}\left(\frac{z_p}{2\exp(\alpha_0)\sigma} + B^{-1/2}\frac{z_p^2}{4\exp(2\alpha_0)}\right) \quad (61)$$

$$\frac{\partial t_p}{\partial\gamma} = -\frac{2lnA}{\gamma^2}A^{2/\gamma}. \quad (62)$$

APPENDIX B
FIRST DERIVATIVE OF p-QUANTILE LIFETIME

In (15), the first derivative of p-quantile lifetime t_p with respect to the parameters is $\nabla t_p = [\frac{\partial t_p}{\partial\alpha_0}, \frac{\partial t_p}{\partial\alpha_1}, \frac{\partial t_p}{\partial\sigma^2}, \frac{\partial t_p}{\partial\gamma}]'$, whose elements are given in (59)–(62), where $A = B^2/4\sqrt{\omega\sigma^2/\exp(3\alpha_0)}$, $B = z_p + \sqrt{4\omega\exp(\alpha_0)/\sigma^2 + z_p^2}$.

REFERENCES

[1] S. G. Chalk and J. F. Miller, "Key challenges and recent progress in batteries, fuel cells, and hydrogen storage for clean energy systems," *J. Power Sources*, vol. 159, no. 1, pp. 73–80, 2006.

[2] E. V. Thomas, I. Bloom, J. P. Christophersen, and V. S. Battaglia, "Statistical methodology for predicting the life of lithium-ion cells via accelerated degradation testing," *J. Power Sources*, vol. 184, no. 1, pp. 312–317, 2008.

[3] F. K. Wang and T. P. Chu, "Lifetime predictions of LED-based light bars by accelerated degradation test," *Microelectron. Rel.*, vol. 52, no. 7, pp. 1332–1336, 2012.

[4] T. Santini *et al.*, "Accelerated degradation data of SiC MOSFETs for lifetime and remaining useful life assessment," *Microelectron. Rel.*, vol. 54, no. 9–10, pp. 1718–1723, 2014.

[5] K. Lin, Y. Chen, and D. Xu, "Reliability assessment model considering heterogeneous population in a multiple stresses accelerated test," *Rel. Eng. Syst. Safety*, vol. 165, pp. 134–143, 2017.

[6] G. A. Whitmore and F. Schenkelberg, "Modelling accelerated degradation data using Wiener diffusion with a time scale transformation," *Lifetime Data Anal.*, vol. 3, no. 1, pp. 27–45, 1997.

[7] C. Park and W. J. Padgett, "Stochastic degradation models with several accelerating variables," *IEEE Trans. Rel.*, vol. 55, no. 2, pp. 379–390, Jun. 2006.

[8] H. Lim and B. J. Yum, "Optimal design of accelerated degradation tests based on Wiener process models," *J. Appl. Statist.*, vol. 38, no. 2, pp. 309–325, 2011.

[9] L. A. Escobar and W. Q. Meeker, "A review of accelerated test models," *Statist. Sci.*, vol. 21, no. 4, pp. 552–577, 2006.

[10] W. B. Nelson, *Accelerated Testing: Statistical Models, Test Plans, and Data Analysis*. New York, NY, USA: Wiley, 1990.

[11] W. Q. Meeker and L. A. Escobar, *Statistical Methods for Reliability Data*. New York, NY, USA: Wiley, 1998.

[12] Z.-S. Ye and M. Xie, "Stochastic modelling and analysis of degradation for highly reliable products (with discussion)," *Appl. Stoch. Model Bus. Ind.*, vol. 31, no. 1, pp. 16–36, 2015.

[13] H. T. Liao and E. A. Elsayed, "Reliability inference for field conditions from accelerated degradation testing," *Nav. Res. Logist.*, vol. 53, no. 6, pp. 576–587, 2006.

[14] Z.-S. Ye, N. Chen, and Y. Shen, "A new class of Wiener process models for degradation analysis," *Rel. Eng. Syst. Safety*, vol. 139, pp. 58–67, 2015.

[15] V. Bagdonavicius and M. S. Nikulin, "Estimation in degradation models with explanatory variables," *Lifetime Data Anal.*, vol. 7, no. 1, pp. 85–103, 2001.

[16] S. T. Tseng, N. Balakrishnan, and C. C. Tsai, "Optimal step-stress accelerated degradation test plan for gamma degradation processes," *IEEE Trans. Rel.*, vol. 58, no. 4, pp. 611–618, Dec. 2009.

[17] M. H. Ling, K. L. Tsui, and N. Balakrishnan, "Accelerated degradation analysis for the quality of a system based on the Gamma process," *IEEE Trans. Rel.*, vol. 64, no. 1, pp. 463–472, Mar. 2015.

[18] H. Lim, "Optimum accelerated degradation tests for the Gamma degradation process case under the constraint of total cost," *Entropy*, vol. 17, pp. 2556–2572, 2015.

[19] X. Wang and D. Xu, "An inverse Gaussian process model for degradation data," *Technometrics*, vol. 52, no. 2, pp. 188–197, 2010.

[20] Z.-S. Ye and N. Chen, "The inverse Gaussian process as a degradation model," *Technometrics*, vol. 56, no. 3, pp. 302–311, 2013.

[21] Z.-S. Ye, L.-P. Chen, L. C. Tang, and M. Xie, "Accelerated degradation test planning using the inverse Gaussian process," *IEEE Trans. Rel.*, vol. 63, no. 3, pp. 750–763, Sep. 2014.

[22] W. W. Peng, Y. F. Li, Y. J. Yang, H. Z. Huang, and M. J. Zuo, "Inverse Gaussian process models for degradation analysis: A Bayesian perspective," *Rel. Eng. Syst. Safety*, vol. 130, pp. 175–189, 2014.

[23] S. Tang, X. Guo, C. Yu, H. Xue, and Z. Zhou, "Accelerated degradation tests modeling based on the nonlinear Wiener process with random effects," *Math. Probl. Eng.*, vol. 2014, 2014, Art. no. 560726,.

[24] X. Wang, N. Balakrishnan, and B. Guo, "Residual life estimation based on a generalized Wiener degradation process," *Rel. Eng. Syst. Safety*, vol. 124, pp. 13–23, 2014.

[25] H.-W. Wang, T.-X. Xu, and W.-Y. Wang, "Remaining life prediction based on Wiener processes with ADT prior information," *Qual. Rel. Eng. Int.*, vol. 32, no. 3, pp. 753–765, 2016.

[26] I. T. Yu and C. L. Chang, "Applying Bayesian model averaging for quantile estimation in accelerated life tests," *IEEE Trans. Rel.*, vol. 61, no. 1, pp. 74–83, Mar. 2012.

[27] C. Park and W. J. Padgett, "Accelerated degradation models for failure based on geometric Brownian motion and Gamma processes," *Lifetime Data Anal.*, vol. 11, no. 4, pp. 511–527, 2005.

[28] Z. Q. Pan and N. Balakrishnan, "Multiple-steps step-stress accelerated degradation modeling based on Wiener and Gamma processes," *Commun. Statist.-Simul. C*, vol. 39, no. 7, pp. 1384–1402, 2010.

[29] K. B. Laskey, "Model uncertainty: Theory and practical implications," *IEEE Trans. Syst., Man, Cybern. A, Syst. Humans*, vol. 26, no. 3, pp. 340–348, May 1996.
[30] T. Nilsen and T. Aven, "Models and model uncertainty in the context of risk analysis," *Rel. Eng. Syst. Safety*, vol. 79, no. 3, pp. 309–317, 2003.
[31] T. Aven and E. Zio, "Some considerations on the treatment of uncertainties in risk assessment for practical decision making," *Rel. Eng. Syst. Safety*, vol. 96, no. 1, pp. 64–74, 2011.
[32] E. Zio and G. E. Apostolakis, "Two methods for the structured assessment of model uncertainty by experts in performance assessments of radioactive waste repositories," *Rel. Eng. Syst. Safety*, vol. 54, no. 2C3, pp. 225–241, 1996.
[33] J. A. Hoeting, D. Madigan, A. E. Raftery, and C. T. Volinsky, "Bayesian model averaging: a tutorial," *Statist. Sci.*, pp. 382–401, 1999.
[34] L. Wasserman, "Bayesian model selection and model averaging," *J. Math. Psychol.*, vol. 44, no. 1, pp. 92–107, 2000.
[35] C. Fernandez, E. Ley, and M. F. Steel, "Benchmark priors for Bayesian model averaging," *J. Econometrics*, vol. 100, no. 2, pp. 381–427, 2001.
[36] I. Park and R. V. Grandhi, "A Bayesian statistical method for quantifying model form uncertainty and two model combination methods," *Rel. Eng. Syst. Safety*, vol. 129, pp. 46–56, 2014.
[37] E. L. Droguett and A. Mosleh, "Bayesian methodology for model uncertainty using model performance data," *Risk Anal.*, vol. 28, no. 5, pp. 1457–1476, 2008.
[38] P. Baraldi and E. Zio, "A comparison between probabilistic and Dempster–Shafer theory approaches to model uncertainty analysis in the performance assessment of radioactive waste repositories," *Risk Anal.*, vol. 30, no. 7, pp. 1139–1156, 2010.
[39] I. Park and R. V. Grandhi, "Quantification of model-form and parametric uncertainty using evidence theory," *Struct. Safety*, vol. 39, pp. 44–51, 2012.
[40] R. Pan, "A Bayes approach to reliability prediction utilizing data from accelerated life tests and field failure observations," *Qual. Rel. Eng. Int.*, vol. 25, no. 2, pp. 229–240, 2009.
[41] L. Z. Wang, R. Pan, X. Y. Li, and T. M. Jiang, "A Bayesian reliability evaluation method with integrated accelerated degradation testing and field information," *Rel. Eng. Syst. Safety*, vol. 112, pp. 38–47, 2013.
[42] M. Musallam, C. Yin, C. Bailey, and C. M. Johnson, "Application of coupled electro-thermal and physics-of-failure-based analysis to the design of accelerated life tests for power modules," *Microelectron. Rel.*, vol. 54, no. 1, pp. 172–181, 2014.
[43] G. Bhattacharyya and A. Fries, "Fatigue failure models—Birnbaum–Saunders vs. inverse Gaussian," *IEEE Trans. Rel.*, vol. R-31, no. 5, pp. 439–441, Dec. 1982.
[44] D. S. Chang and L. C. Tang, "Percentile bounds and tolerance limits for the Birnbaum–Saunders distribution," *Commun. Statist.-Theory Methods*, vol. 23, no. 10, pp. 2853–2863, 1994.
[45] Y. L. Lio, J. C. Lu, and L. Ruan, "Robust parameter design for quality and reliability issues based on accelerated degradation measurements," *IEEE Trans. Rel.*, vol. 64, no. 3, pp. 949–959, Sep. 2015.
[46] C. C. Tsai and C. T. Lin, "Lifetime inference for highly reliable products based on skew-normal accelerated destructive degradation test model," *IEEE Trans. Rel.*, vol. 64, no. 4, pp. 1340–1355, Dec. 2015.
[47] I. Ntzoufras, *Bayesian Modeling Using WinBUGS*. New York, NY, USA: Wiley, 2011, vol. 698.
[48] L. Liu, X.-Y. Li, T.-M. Jiang, and F.-Q. Sun, "Utilizing accelerated degradation and field data for life prediction of highly reliable products," *Qual. Rel. Eng. Int.*, vol. 32, no. 7, pp. 2281–2297, 2016.
[49] A. E. Raftery, D. Madigan, and J. A. Hoeting, "Bayesian model averaging for linear regression models," *J. Amer. Statist. Assoc.*, vol. 92, no. 437, pp. 179–191, 1997.
[50] G. Yang, *Life Cycle Reliability Engineering*. New York, NY, USA: Wiley, 2007.
[51] M. Abramowitz and I. A. Stegun, *Handbook of Mathematical Functions: With Formulas, Graphs, and Mathematical Tables*. North Chelmsford, MA, USA: Courier, 1964, no. 55.
[52] R. S. Chhikara and J. L. Folks, *The Inverse Gaussian Distribution: Theory, Methodology, And applications*. New York, NY, USA: CRC Press, 1988, vol. 95.

Le Liu received the Bachelor's degree in quality and reliability engineering and the Ph.D. degree in systems engineering from Beihang University, Beijing, China, in 2012 and 2017, respectively.

He is currently a Reliability Engineer at Huawei Institute in Beijing, China. His current research interests include reliability tests and Prognostics and Health Management (PHM).

Xiao-Yang Li received the Ph.D. degree in aerospace systems engineering from Beihang University, Beijing, China, in 2007.

She is currently an Associate Professor in the School of Reliability and Systems Engineering, Beihang University. Her research interests include accelerated testing, prediction technology, and imprecise probability modeling.

Enrico Zio (M'06–SM'09) received the M.Sc. degree in nuclear engineering from the Politecnico di Milano, Milano, Italy, in 1991, the M.Sc. degree in mechanical engineering from the University of California, Los Angeles, Los Angeles, CA, USA, in 1995, and the Ph.D. degrees in nuclear engineering from Politecnico di Milano and Massachusetts Institute of Technology, Cambridge, MA, USA, in 1996 and 1998, respectively.

He is currently a Director of the Chair on Systems Science and the Energetic Challenge of the Foundation Electricite de France, CentraleSupelec, Universite Paris-Saclay, Paris, France, a Full Professor at Politecnico di Milano, an Adjunct Professor at the University of Stavanger, Stavanger, Norway, City University of Hong Kong, Kowloon Tong, Hong Kong, Beihang University, Beijing, China, Wuhan University, Hubei, China, and the Co-Director of the Center of Resilience and Safety for Critical Infrastructures, Beijing, China. His research focuses on the modeling of the failure–repair–maintenance behavior of components and complex systems, for their reliability, maintainability, prognostics, safety, vulnerability, and security analysis, and on Monte Carlo simulation methods, soft computing techniques, and optimization heuristics.

Rui Kang received the Bachelor's and Master's degrees in electrical engineering from Beihang University, Beijing, China, in 1987 and 1990, respectively.

He is currently a Distinguished Professor in the School of Reliability and Systems Engineering, Beihang University, Beijing, China. His main research interests include reliability and resilience for complex system and modeling epistemic uncertainty in reliability and maintainability.

Prof. Kang is currently an Associate Editor of the IEEE TRANSACTIONS ON RELIABILITY, *Proceedings of the Institution of Mechanical Engineers, Part O: Journal of Risk and Reliability*, and *Chinese Journal of Aeronautics*, and he is the founder of the China Prognostics and Health Management Society.

Tong-Min Jiang received the Master's degree in reliability engineering from Beihang University, Beijing, China, in 1990.

He is currently an Eminent Professor in the School of Reliability and Systems Engineering, Beihang University. His research interests include reliability testing and environment engineering of product.